Electronic Transactions on Numerical Analysis.
Volume 46, pp. 71–88, 2017.

ISSN 1068–9613.

ETNA
Kent State University and
Johann Radon Institute (RICAM)

APPLICATION OF THE COLLOCATION METHOD WITH B-SPLINES TO THE GEW EQUATION*

HALIL ZEYBEK† AND S. BATTAL GAZI KARAKOÇ‡

Abstract. In this paper, the generalized equal width (GEW) wave equation is solved numerically by using a quintic B-spline collocation algorithm with two different linearization techniques. Also, a linear stability analysis of the numerical scheme based on the von Neumann method is investigated. The numerical algorithm is applied to three test problems consisting of a single solitary wave, the interaction of two solitary waves, and a Maxwellian initial condition. In order to determine the performance of the numerical method, we compute the error in the L_2- and L_∞-norms and in the invariants I_1, I_2, and I_3 of the GEW equation. These calculations are compared with earlier studies. Afterwards, the motion of solitary waves according to different parameters is designed.

Key words. GEW equation, finite element method, quintic B-spline, soliton, solitary waves

AMS subject classifications. 41A15, 65N30, 76B25

1. Introduction.

This work is concerned with the numerical investigation of the following generalized equal width (GEW) wave equation:

$$U_t + \varepsilon U^p U_x - \mu U_{xxt} = 0, \tag{1.1}$$

where p is a positive integer, ε and μ are positive constants, t is time and x is the space coordinate, equipped with physical boundary conditions $U \to 0$ as $x \to \pm\infty$. For this study, we consider $x \in [a, b]$, and the boundary and initial conditions are assumed to be of the form

$$\begin{aligned} U(a,t) &= 0, \qquad U(b,t) = 0, \qquad t > 0, \\ U_x(a,t) &= 0, \qquad U_x(b,t) = 0, \qquad t > 0, \\ U(x,0) &= f(x), \qquad\qquad\quad a \le x \le b, \end{aligned} \tag{1.2}$$

where $f(x) \in C([a, b])$ is a prescribed function, which will be defined in the later sections depending on the test problems. The form of the initial pulse will be chosen so that at large distances from the pulse, $|U|$ is extremely small and essentially attains the free space boundary condition $U = 0$. For fluid problems, the quantity U describes the wave amplitude of the water surface or a similar physical quantity. On the other hand, in plasma applications, it is related to the negative of the electrostatic potential.

The GEW equation was firstly introduced by Peregrine [18] and Benjamin et al. [1] as a model for small-amplitude long waves on the surface of water in a channel. Equation (1.1), which is an alternative model to the generalized regularized long wave (GRLW) equation and the generalized Korteweg-de Vries (GKdV) equation, is based upon the equal width wave (EW) equation. These general equations are nonlinear wave equations with a $(p + 1)$st nonlinearity, and they allow for solitary solutions, which are pulse-like [21]. Hence, solitary wave solutions of these equations illuminate many important physical phenomena.

The numerical solution of the GEW equation has been studied in the recent years. The quadratic and cubic B-spline collocation method was applied to the GEW equation by Evans and Raslan [4] and Raslan [21]. Roshan has solved the equation by using the Petrov-Galerkin

*Received January 8, 2016. Accepted January 30, 2017. Published online on March 8, 2017. Recommended by Johannes Kraus.

†Department of Applied Mathematics, Faculty of Computer Science, Abdullah Gul University, 38080 Kayseri, Turkey (zeybek.halil45@gmail.com).

‡Department of Mathematics, Faculty of Science and Art, Nevsehir Haci Bektas Veli University, 50300 Nevsehir, Turkey (sbgkarakoc@nevsehir.edu.tr).

ETNA
Kent State University and
Johann Radon Institute (RICAM)

method [24]. Panahipour has employed the RBF collocation method for the numerical treatment of the GEW equation [17]. Also, exact solution techniques have been presented by Hamdi et al. [9] and Taghizadeh et al. [29].

In the case of $p = 1$, the obtained equation is called the equal width wave (EW) equation. The EW equation plays an important role in the motion of nonlinear dispersive waves such as shallow water waves or ion acoustic plasma waves. Up to now, many numerical and exact solution methods have been implemented for the EW equation. Gardner and Gardner [6] and Gardner et al. [7] applied the Galerkin method and the Petrov-Galerkin method to the EW equation. A least-squares finite element scheme for the EW equation was used by Zaki [30]. Collocation method based on cubic, quartic, and septic B-spline functions has been investigated for the numerical solution of the EW equation by Dag and Saka [2], Raslan [20], and Fazal-i-Haq et al. [5]. For $p = 2$, the modified equal width wave (MEW) equation is obtained. The MEW equation has been solved numerically by using finite element methods [3, 8, 10, 12, 26].

Collocation methods based on B-spline functions have been investigated by many researchers for getting a numerical solution of the nonlinear equations. A cubic collocation method was applied to the MRLW equation by Khalifa et al. [15]. RLW, MRLW, and Kawahara equations were solved by using septic B-spline collocation schemes [11, 14, 28]. Quintic B-spline collocation methods have been used for the numerical solution of the KdVB, RLW, MRLW, General Rosenau-RLW, and the coupled KDV equation by Zaki [31], Saka et al. [27], Raslan and EL-Danaf [22], Mittal and Jain [16], Karakoç et al. [13], and Raslan et al. [23].

In this work, a quintic B-spline collocation method is implemented for the GEW equation with two different linearization techniques. This work is designed as follows: the collocation method based on quintic B-spline functions is presented in Section 2. In Section 3, a linear stability analysis is performed. Numerical examples and results are presented in Section 4. In the last Section 5, a conclusion is given.

2. The quintic B-spline collocation method. We partition the interval $[a, b]$ into finite elements of uniform length h by the knots x_m such that $a = x_0 < x_1 < \ldots < x_N = b$ and $h = (x_{m+1} - x_m)$. The quintic B-spline functions $\phi_m(x)$, $m = -2, -1, ..., N + 2$, at the knots x_m, which form a basis for functions (especially for $U_N(x, t)$) defined on the solution region $[a, b]$, are given in [19] by Prenter

$$\phi_m(x) = \frac{1}{h^5} \begin{cases} (x - x_{m-3})^5, & [x_{m-3}, x_{m-2}) \\ (x - x_{m-3})^5 - 6(x - x_{m-2})^5, & [x_{m-2}, x_{m-1}) \\ (x - x_{m-3})^5 - 6(x - x_{m-2})^5 + 15(x - x_{m-1})^5, & [x_{m-1}, x_m) \\ (x_{m+3} - x)^5 - 6(x_{m+2} - x)^5 + 15(x_{m+1} - x)^5, & [x_m, x_{m+1}) \\ (x_{m+3} - x)^5 - 6(x_{m+2} - x)^5, & [x_{m+1}, x_{m+2}) \\ (x_{m+3} - x)^5, & [x_{m+2}, x_{m+3}] \\ 0, & \text{otherwise.} \end{cases} \tag{2.1}$$

Each quintic B-spline ϕ_m covers 6 elements so that each finite element $[x_m, x_{m+1}]$ is covered by 6 splines. The numerical approximation $U_N(x, t)$ to the exact solution $U(x, t)$ of equation (1.1) is written in terms of the quintic B-splines as

$$U_N(x, t) = \sum_{m=-2}^{N+2} \phi_m(x)\delta_m(t), \tag{2.2}$$

in which the unknown functions $\delta_m(t)$ will be found by using the boundary and collocation conditions. By substituting the quintic B-spline functions (2.1) into the approximate function (2.2), the nodal values of U_m, U'_m, U''_m are obtained in terms of the time functions δ_m by

ETNA
Kent State University and
Johann Radon Institute (RICAM)

$$
\begin{aligned}
U_m(t) &:= U_N(x_m,t) = \delta_{m-2} + 26\delta_{m-1} + 66\delta_m + 26\delta_{m+1} + \delta_{m+2},\\
U'_m(t) &:= \partial_x U_N(x_m,t) = \frac{5}{h}\left(-\delta_{m-2} - 10\delta_{m-1} + 10\delta_{m+1} + \delta_{m+2}\right),\\
U''_m(t) &:= \partial_{xx} U_N(x_m,t) = \frac{20}{h^2}(\delta_{m-2} + 2\delta_{m-1} - 6\delta_m + 2\delta_{m+1} + \delta_{m+2}).
\end{aligned} \tag{2.3}
$$

Here, the finite elements are represented by the intervals $[x_m, x_{m+1}]$, and the function $U_N(x,t)$ on the element $[x_m, x_{m+1}]$ is given by

$$U_N(x,t) = \sum_{j=m-2}^{m+3} \phi_j(x)\delta_j(t).$$

In the first linearization technique, the expression U^p in the nonlinear term U^pU_x is taken as

$$Z_m = (U_m)^p = (\delta_{m-2} + 26\delta_{m-1} + 66\delta_m + 26\delta_{m+1} + \delta_{m+2})^p.$$

In the second (Rubin and Graves) linearization technique, the expression $U^{p-1}U_x$ in the nonlinear term U^pU_x is taken as

$$Z_m = (U_m)^{p-1}U'_m.$$

Applying the Rubin and Graves linearization technique [25] to the $U^{p-1}U_x$-term, we obtain the following equality

$$
\begin{aligned}
\left((U_m)^{p-1}U'_m\right)^{n+1} = &\left((U_m)^{p-1}\right)^n (U'_m)^{n+1}\\
&+ \left((U_m)^{p-1}\right)^{n+1}(U'_m)^n - \left((U_m)^{p-1}\right)^n (U'_m)^n.
\end{aligned}
$$

For both linearization techniques, it is assumed that Z_m is locally a constant. When we use the nodal values of U_m and its spatial derivatives given by (2.3) in equation (1.1), then for the first linearization technique, we get the following set of the coupled ordinary differential equations:

$$
\begin{aligned}
&\dot\delta_{m-2} + 26\dot\delta_{m-1} + 66\dot\delta_m + 26\dot\delta_{m+1} + \dot\delta_{m+2}\\
&\quad + \frac{5\varepsilon Z_m}{h}(-\delta_{m-2} - 10\delta_{m-1} + 10\delta_{m+1} + \delta_{m+2})\\
&\quad - \frac{20\mu}{h^2}(\dot\delta_{m-2} + 2\dot\delta_{m-1} - 6\dot\delta_m + 2\dot\delta_{m+1} + \dot\delta_{m+2}) = 0,
\end{aligned} \tag{2.4}
$$

where

$$Z_m = (U_m)^p.$$

For the second linearization technique, we obtain the following form:

$$
\begin{aligned}
&\dot\delta_{m-2} + 26\dot\delta_{m-1} + 66\dot\delta_m + 26\dot\delta_{m+1} + \dot\delta_{m+2}\\
&\quad + \varepsilon Z_m(\delta_{m-2} + 26\delta_{m-1} + 66\delta_m + 26\delta_{m+1} + \delta_{m+2})\\
&\quad - \frac{20\mu}{h^2}(\dot\delta_{m-2} + 2\dot\delta_{m-1} - 6\dot\delta_m + 2\dot\delta_{m+1} + \dot\delta_{m+2}) = 0,
\end{aligned} \tag{2.5}
$$

where

$$Z_m = (U_m)^{p-1}U'_m$$

ETNA
Kent State University and
Johann Radon Institute (RICAM)

and the dot "˙" denotes the time-derivative. If δ_i and its time-derivatives $\dot{\delta}_i$ in equations (2.4) and (2.5) are discretized by the Crank-Nicolson formula or by a forward difference approach, then

$$\delta_m = \frac{1}{2}(\delta_m^n + \delta_m^{n+1}), \qquad \dot{\delta}_m = \frac{\delta_m^{n+1} - \delta_m^n}{\Delta t}, \qquad \delta_m^n := \delta_m(t_n),$$

respectively. For the first linearization approach, we get a recurrence relationship between the two time levels at iteration n and $n+1$ relating the two unknown functions δ_i^{n+1}, δ_i^n, for $i = m-2, ..., m+2$,

$$\begin{aligned}\gamma_1\delta_{m-2}^{n+1} + \gamma_2\delta_{m-1}^{n+1} + \gamma_3\delta_m^{n+1} + \gamma_4\delta_{m+1}^{n+1} + \gamma_5\delta_{m+2}^{n+1} \\ = \gamma_5\delta_{m-2}^n + \gamma_4\delta_{m-1}^n + \gamma_3\delta_m^n + \gamma_2\delta_{m+1}^n + \gamma_1\delta_{m+2}^n,\end{aligned} \tag{2.6}$$

where

$$\begin{aligned}&\gamma_1 = (1 - EZ_m - M), && \gamma_2 = (26 - 10EZ_m - 2M), && \gamma_3 = (66 + 6M),\\ &\gamma_4 = (26 + 10EZ_m - 2M), && \gamma_5 = (1 + EZ_m - M), &&\\ &m = 0, 1, \ldots, N, && E = \frac{5\varepsilon}{2h}\Delta t, && M = \frac{20\mu}{h^2}.\end{aligned}$$

For the second linearization technique, the recurrence relationship has been obtained as follows:

$$\begin{aligned}\beta_1\delta_{m-2}^{n+1} + \beta_2\delta_{m-1}^{n+1} + \beta_3\delta_m^{n+1} + \beta_2\delta_{m+1}^{n+1} + \beta_1\delta_{m+2}^{n+1} \\ = \beta_4\delta_{m-2}^n + \beta_5\delta_{m-1}^n + \beta_6\delta_m^n + \beta_5\delta_{m+1}^n + \beta_4\delta_{m+2}^n,\end{aligned} \tag{2.7}$$

where

$$\begin{aligned}&\beta_1 = (1 + KZ_m - R), && \beta_2 = (26 + 26KZ_m - 2R), && \beta_3 = (66 + 66KZ_m + 6R),\\ &\beta_4 = (1 - KZ_m - R), && \beta_5 = (26 - 26KZ_m - 2R), && \beta_6 = (66 - 66KZ_m + 6R),\\ &m = 0, 1, \ldots, N, && K = \frac{\varepsilon\Delta t}{2}, && R = \frac{20\mu}{h^2}.\end{aligned}$$

Obviously, the recurrence relations (2.6) and (2.7) comprise of $(N+1)$ linear equations. To achieve a unique solution for this system involving the $(N+5)$ unknowns $(\delta_{-2}, \delta_{-1}, \ldots, \delta_{N+1}, \delta_{N+2})^T$, four additional constraints are needed. For this, we use the boundary conditions (1.2) and efface δ_{-2}, δ_{-1} and $\delta_{N+1}, \delta_{N+2}$ from the systems (2.6) and (2.7). In this case, we get a matrix equation including the $N+1$ unknown functions $\mathbf{d^n} = (\delta_0, \delta_1, \ldots, \delta_N)^T$ of the form

$$A\mathbf{d^{n+1}} = B\mathbf{d^n}.$$

The matrices A and B are banded nearly diagonal $(N+1) \times (N+1)$ matrices with five columns element (called a penta-diagonal matrix). This matrix equation can be solved by using the penta-diagonal algorithm (see Section 2.1).

In this solution process, the functions δ^{n+1} at various time-steps is calculated from the iterations (2.6) and (2.7). Before proceeding to the next time step, to cope with the nonlinearity caused by Z_m, the new time functions in Z_m are calculated by $(\delta^*)^{n+1} = \delta^n + \frac{1}{2}(\delta^{n+1} - \delta^n)$ (as used in [26, 27]). This inner iteration is applied two or three times to achieve a better result

ETNA
Kent State University and
Johann Radon Institute (RICAM)

at each time step. In order to initiate the recurrence relation, the initial functions $\mathbf{d^0}$ must be calculated from the initial condition and the derivatives at the boundaries:

$$\begin{aligned} U(x_m,0) &= f(x_m), && && m = 0,1,2,...,N,\\ (U_N)_x(a,0) &= 0, && (U_N)_x(b,0) = 0,\\ (U_N)_{xx}(a,0) &= 0, && (U_N)_{xx}(b,0) = 0. \end{aligned}$$

This yields the matrix equation for the initial vector $\mathbf{d^0}$,

$$W\mathbf{d^0} = b,$$

where

$$W = \begin{bmatrix} 54 & 60 & 6 & & & & & \\ 25.25 & 67.5 & 26.25 & 1 & & & & \\ 1 & 26 & 66 & 26 & 1 & & & \\ & & \ddots & \ddots & \ddots & \ddots & & \\ & & & 1 & 26 & 66 & 26 & 1 \\ & & & & 1 & 26.25 & 67.5 & 25.25 \\ & & & & & 6 & 60 & 54 \end{bmatrix},$$

$$\mathbf{d^0} = (\delta_0, \delta_1, \delta_2, ..., \delta_{N-2}, \delta_{N-1}, \delta_N)^T, \qquad \text{and}$$

$$b = (U(x_0,0), U(x_1,0), ..., U(x_{N-1},0), U(x_N,0))^T.$$

2.1. The solution by the penta-diagonal algorithm. As used in the Fortran program, the solution method by the penta-diagonal algorithm is explained as follows: the penta-diagonal system can be written as

$$a_i\delta_{i-2} + b_i\delta_{i-1} + c_i\delta_i + d_i\delta_{i+1} + e_i\delta_{i+2} = f_i, \qquad i = 0, 1, \cdots, N.$$

In the first step, the parameters are initialized with

$$\begin{aligned} &\alpha_0 = 0, \quad \beta_0 = c_0, && \mu_0 = \frac{d_0}{\beta_0}, && \zeta_0 = \frac{e_0}{\beta_0}, \quad \lambda_0 = \frac{f_0}{\beta_0},\\ &\alpha_1 = b_0, \quad \beta_1 = c_1 - \alpha_1\mu_0, && \mu_1 = \frac{d_1 - \alpha_1\zeta_0}{\beta_1}, && \zeta_1 = \frac{e_1}{\beta_1}, \quad \lambda_1 = \frac{f_1 - \alpha_1\lambda_0}{\beta_1}. \end{aligned}$$

Secondly, the following parameters are computed

$$\begin{aligned} &\alpha_i = b_{i-1} - a_{i-2}\mu_{i-2}, \quad \beta_i = c_i - \alpha_i\mu_{i-1} - a_{i-2}\zeta_{i-2}, \quad \mu_i = \frac{d_i - \alpha_i\zeta_{i-1}}{\beta_i},\\ &\zeta_i = \frac{e_i}{\beta_i}, \qquad \lambda_i = \frac{f_i - \alpha_i\lambda_{i-1} - a_{i-2}\lambda_{i-2}}{\beta_i}, \qquad \text{for } i = 2, 3, \ldots, N. \end{aligned}$$

Now we achieve the solution

$$\begin{aligned} \delta_i &= \lambda_i - \zeta_i\delta_{i+2} - \mu_i\delta_{i+1}, && i = 0, 1, \ldots, N-3, N-2,\\ \delta_{N-1} &= \lambda_{N-1} - \mu_{N-1}\delta_N, \qquad \delta_N = \lambda_N. \end{aligned}$$

ETNA
Kent State University and
Johann Radon Institute (RICAM)

3. A linear stability analysis. In order to investigate the linear stability of the numerical scheme, we use the von Neumann approach and assume that the quantity U^p in the nonlinear term U^pU_x of the GEW equation is locally constant. Then, we substitute the Fourier mode $\delta_m^n = \xi^n e^{imkh}$, $(i = \sqrt{-1})$, in which k is a mode number and h is the element size, into (2.6), which yields the following equality

$$\begin{aligned}(3.1)\qquad &\gamma_1\xi^{n+1}e^{i(m-2)kh} + \gamma_2\xi^{n+1}e^{i(m-1)kh} + \gamma_3\xi^{n+1}e^{imkh} \\ &\quad + \gamma_4\xi^{n+1}e^{i(m+1)kh} + \gamma_5\xi^{n+1}e^{i(m+2)kh} \\ &= \gamma_5\xi^{n}e^{i(m-2)kh} + \gamma_4\xi^{n}e^{i(m-1)kh} + \gamma_3\xi^{n}e^{imkh} \\ &\quad + \gamma_2\xi^{n}e^{i(m+1)kh} + \gamma_1\xi^{n}e^{i(m+2)kh}.\end{aligned}$$

Applying Euler's formula ($e^{ikh} = \cos(kh) + i\sin(kh)$) to the equation (3.1) leads to the following growth factor ξ:

$$\xi = \frac{a - ib}{a + ib},$$

where

$$\begin{aligned}a &= \gamma_3 + (\gamma_4 + \gamma_2)\cos[hk] + (\gamma_5 + \gamma_1)\cos[2hk], \\ b &= (\gamma_4 - \gamma_2)\sin[hk] + (\gamma_5 - \gamma_1)\sin[2hk].\end{aligned}$$

The modulus of $|\xi|$ is 1. This means that the linearized scheme is unconditionally stable.

4. Numerical examples and results. In this section, the numerical algorithm is applied to the following three test problems: the motion of a single solitary wave, the interaction of two solitary waves, and a Maxwellian initial condition. The variations of the invariants (4.2) are calculated to verify the conservation properties of the numerical approach. In order to demonstrate the accuracy of the numerical scheme and compare our results with other ones given in the literature, the L_2- and L_∞-error norms are calculated by using the analytical solution in (4.1). The errors in the L_2- and L_∞-norms are given as follows:

$$\begin{aligned}L_2 &= \left\|U^{exact} - U_N\right\|_2 \simeq \sqrt{h\sum_{j=0}^{N}\left|U_j^{exact} - (U_N)_j\right|^2}, \\ L_\infty &= \left\|U^{exact} - U_N\right\|_\infty \simeq \max_j\left|U_j^{exact} - (U_N)_j\right|.\end{aligned}$$

The analytic solution of the GEW equation (1.1) given in [4, 21] is

$$(4.1)\qquad U(x,t) = \sqrt[p]{\frac{c(p+1)(p+2)}{2\varepsilon}\operatorname{sech}^2\left[\frac{p}{2\sqrt{\mu}}(x - ct - x_0)\right]},$$

where c is the the constant velocity of the wave travelling in the positive direction of the x-axis and x_0 is an arbitrary constant. Three invariants of motion which correspond to the conservation of mass, momentum, and energy are given as

$$(4.2)\qquad I_1 = \int_a^b U\,dx, \qquad I_2 = \int_a^b \left[U^2 + \mu U_x^2\right]dx, \qquad I_3 = \int_a^b U^{p+2}dx.$$

ETNA
Kent State University and
Johann Radon Institute (RICAM)

4.1. The motion of a single solitary wave. As a first example, we consider the GEW equation (1.1) with the initial condition obtained by taking $t = 0$ in (4.1). Applying the numerical approach with the two different linearization techniques, the changes in the conservative quantities and the values of the error norms are calculated from time $t = 0$ to $t = 20$. For this, we have constructed five sets of parameters by taking different values of p, c and the amplitute amp $:= \sqrt[p]{\frac{c(p+1)(p+2)}{2\varepsilon}}$ and the same values of $h = 0.1$, $\Delta t = 0.2$, $\varepsilon = 3$, $\mu = 1$, $x_0 = 30$, $0 \le x \le 80$.

In the first case, we take the parameters $p = 2$, $c = 1/32$, and $c = 1/2$. These yield amp $= 0.25$ and amp $= 1$. The obtained results are tabulated in Table 4.1 and Table 4.2. It is observed from Table 4.1 that the values of the invariants are nearly the same as the time increases. Table 4.2 shows that the changes of the invariants from their initial values are less than 0.009%, 0.03%, 0.03%, respectively. Also, we have found that the magnitude of the error norms L_2 and L_∞ is quite small for each linearization technique, as expected.

TABLE 4.1
Errors and invariants for single solitary wave with $p = 2, amp = 0.25, h = 0.1, \Delta t = 0.2, x \in [0, 80]$.

t		0	5	10	15	20
I_1	First	0.7853966	0.7853966	0.7853965	0.7853965	0.7853965
	Second	0.7853966	0.7853966	0.7853966	0.7853966	0.7853966
I_2	First	0.1666664	0.1666663	0.1666663	0.1666663	0.1666663
	Second	0.1666664	0.1666664	0.1666664	0.1666664	0.1666664
I_3	First	0.0052083	0.0052083	0.0052083	0.0052083	0.0052083
	Second	0.0052083	0.0052083	0.0052083	0.0052083	0.0052083
$L_2\times10^5$	First	0.00000000	0.03366038	0.06865677	0.10532104	0.14404828
	Second	0.00000000	0.03127090	0.06398038	0.09850392	0.13526316
$L_\infty\times10^5$	First	0.00000000	0.02509311	0.05215679	0.08029086	0.10853345
	Second	0.00000000	0.02105067	0.04383634	0.06759518	0.09151024

TABLE 4.2
Errors and invariants for single solitary wave with $p = 2, amp = 1, h = 0.1, \Delta t = 0.2, x \in [0, 80]$.

t		0	5	10	15	20
I_1	First	3.1415863	3.1373888	3.1332323	3.1291144	3.1250343
	Second	3.1415863	3.1416080	3.1416294	3.1416508	3.1416722
I_2	First	2.6666616	2.6610537	2.6555067	2.6500168	2.6445829
	Second	2.6666616	2.6667229	2.6667836	2.6668444	2.6669051
I_3	First	1.3333283	1.3277256	1.3221957	1.3167341	1.3113394
	Second	1.3333283	1.3333895	1.3334503	1.3335110	1.3335718
L_2	First	0.00000000	0.00665826	0.01742910	0.03232178	0.05132106
	Second	0.00000000	0.00419982	0.00841618	0.01260569	0.01675092
L_∞	First	0.00000000	0.00474985	0.01201728	0.02183195	0.03416753
	Second	0.00000000	0.00259399	0.00517928	0.00773610	0.01026391

Secondly, if $p = 3$, $c = 0.001$, and $c = 0.3$, then the values amp $= 0.15$ and amp $= 1$ are obtained. The numerical results are reported in Table 4.3 and Table 4.4. As can be seen

ETNA
Kent State University and
Johann Radon Institute (RICAM)

TABLE 4.3
Errors and invariants for single solitary wave with $p = 3, amp = 0.15$, $h = 0.1$, $\Delta t = 0.2$, $x \in [0, 80]$.

t		0	5	10	15	20
I_1	First	0.4189154	0.4189154	0.4189154	0.4189154	0.4189154
	Second	0.4189154	0.4189154	0.4189154	0.4189154	0.4189154
I_2	First	0.0549807	0.0549807	0.0549807	0.0549807	0.0549807
	Second	0.0549807	0.0549807	0.0549807	0.0549807	0.0549807
$I_3 \times 10^4$	First	0.0000733	0.0000733	0.0000733	0.0000733	0.0000733
	Second	0.0000733	0.0000733	0.0000733	0.0000733	0.0000733
$L_2 \times 10^7$	First	0.00000000	0.04797509	0.09597025	0.14398271	0.19200973
	Second	0.00000000	0.04795135	0.09592277	0.14391151	0.19191480
$L_\infty \times 10^7$	First	0.00000000	0.05730697	0.11490440	0.17357780	0.23297300
	Second	0.00000000	0.05727720	0.11485490	0.17350253	0.23287122

in Table 4.3, the three invariants are nearly unchanged as the time increases. In Table 4.4, the changes in the invariants from their initial value are less than 0.007%, 0.02% and 0.02%, respectively. In addition, the values of the error in the L_2- and L_∞-norms are adequately small for both linearization techniques.

Finally, we choose the quantities $p = 4$, $c = 0.2$. This leads to amp $= 1$. The obtained results are given in Table 4.5 which clearly shows that the changes of the invariants are less than 0.02%, 0.03% and 0.03%. Besides, we observed that the error in the L_2- and L_∞-norm is reasonably small.

On the other hand, to investigate the values of the error norms at different time and space steps, we use the parameters $p = 2, 3, 4, 6, 8, 10$ and $c = 0.03, 0.1, 0.3$ with $\varepsilon = 3$, $\mu = 1$, $x_0 = 30$, $x \in [0, 80]$. The associated computational data are presented in Table 4.6 and Table 4.7, which indicate that the error norms become smaller with finer space and time grids and increases with p and c. The motion of a single solitary wave is displayed at times $t = 0, 10, 20$ in Figure 4.1. As can be seen in this figure, the solitary wave moves to the right at nearly unchanged speed and conserves its amplitude and shape as the time proceeds. Increasing the value of p raises the peak position of the single solitary wave.

Table 4.8 gives a comparison of our numerical results with the ones obtained by earlier studies [3, 4, 10, 12, 21, 24]. It is clearly seen from this table that the three conserved quantities are very similar for each method. The magnitude of error norms found by our numerical scheme is smaller than the others for $p = 2, 3$, and it is almost the same as in [24] for $p = 4$.

4.2. The interaction of two solitary waves. In the second test problem, we investigate the interaction of two positive solitary waves by using the following initial condition

$$U(x,0) = \sum_{i=1}^{2} \sqrt[p]{\frac{c_i(p+1)(p+2)}{2\varepsilon}} \operatorname{sech}^2\left[\frac{p}{2\sqrt{\mu}}(x - x_i)\right], \tag{4.3}$$

where c_i and x_i, $i = 1, 2$ are arbitrary constants. Equation (4.3) provides two solitary waves having different amplitudes of magnitudes 1 and 0.5. at the same direction. Three sets of parameters are considered by taking different values of p, c_i and the same values of $h = 0.1$, $\Delta t = 0.025$, $\varepsilon = 3$, $\mu = 1$, $x_1 = 15, x_2 = 30, 0 \le x \le 80$.

Firstly, we take $p = 2$, $c_1 = 0.5$, and $c_2 = 0.125$. The simulations are done up to time $t = 60$. The quantities of the invariants are reported in Table 4.9, which shows that the variations of the invariants from time $t = 0$ to time $t = 60$ are less than 0.0007%, 0.002%,

ETNA
Kent State University and
Johann Radon Institute (RICAM)

TABLE 4.4
Errors and invariants for single solitary wave with $p = 3, amp = 1, h = 0.1, \Delta t = 0.2, x \in [0, 80]$.

	t	0	5	10	15	20
I_1	First	2.8043580	2.8043577	2.8043575	2.8043572	2.8043570
	Second	2.8043580	2.8043425	2.8043265	2.8043104	2.8042943
I_2	First	2.4639101	2.4639097	2.4639093	2.4639090	2.4639086
	Second	2.4639101	2.4638708	2.4638304	2.4637900	2.4637495
I_3	First	0.9855618	0.9855613	0.9855609	0.9855606	0.9855602
	Second	0.9855618	0.9855224	0.9854821	0.9854416	0.9854011
L_2	First	0.00000000	0.00204427	0.00404918	0.00603437	0.00801470
	Second	0.00000000	0.00166962	0.00341489	0.00522937	0.00708553
L_∞	First	0.00000000	0.00145300	0.00275623	0.00406885	0.00538237
	Second	0.00000000	0.00114839	0.00234552	0.00356458	0.00480470

TABLE 4.5
Errors and invariants for single solitary wave with $p = 4, amp = 1, h = 0.1, \Delta t = 0.2, x \in [0, 80]$.

	t	0	5	10	15	20
I_1	First	2.6220516	2.6220514	2.6220512	2.6220510	2.6220508
	Second	2.6220516	2.6220211	2.6219902	2.6219593	2.6219284
I_2	First	2.3561914	2.3561911	2.3561907	2.3561904	2.3561901
	Second	2.3561914	2.3561273	2.3560625	2.3559975	2.3559327
I_3	First	0.7853952	0.7853948	0.7853945	0.7853942	0.7853939
	Second	0.7853952	0.7853310	0.7852662	0.7852013	0.7851364
L_2	First	0.00000000	0.00106260	0.00211868	0.00316779	0.00421697
	Second	0.00000000	0.00075110	0.00156412	0.00244690	0.00339086
L_∞	First	0.00000000	0.00079729	0.00152151	0.00224723	0.00297952
	Second	0.00000000	0.00055248	0.00115512	0.00179553	0.00247031

TABLE 4.6
Errors for single solitary wave with $t = 20, x \in [0, 80]$.

			p=2			p=3			p=4		
		c	0.03	0.1	0.3	0.03	0.1	0.3	0.03	0.1	0.3
		amp	0.24	0.44	0.77	0.46	0.69	1.00	0.62	0.84	1.10
	h	Δt									
	0.1	0.01	0.0005	0.005	0.051	0.001	0.009	0.082	0.004	0.014	0.111
L_2	0.2	0.01	0.0039	0.014	0.036	0.024	0.063	0.144	0.080	0.183	0.426
$\times$	0.1	0.05	0.0005	0.008	0.221	0.001	0.018	0.494	0.004	0.031	0.837
10^3	0.2	0.05	0.0039	0.016	0.198	0.024	0.069	0.537	0.080	0.195	1.120
	0.1	0.2	0.0011	0.064	2.878	0.003	0.178	7.085	0.008	0.327	14.165
	0.1	0.01	0.0003	0.003	0.035	0.002	0.006	0.058	0.006	0.008	0.080
L_∞	0.2	0.01	0.0047	0.011	0.026	0.032	0.053	0.115	0.117	0.162	0.355
$\times$	0.1	0.05	0.0003	0.005	0.140	0.002	0.012	0.338	0.006	0.020	0.601
10^3	0.2	0.05	0.0047	0.013	0.129	0.032	0.059	0.381	0.117	0.174	0.849
	0.1	0.2	0.0008	0.040	1.775	0.003	0.122	4.804	0.009	0.239	10.250

ETNA
Kent State University and
Johann Radon Institute (RICAM)

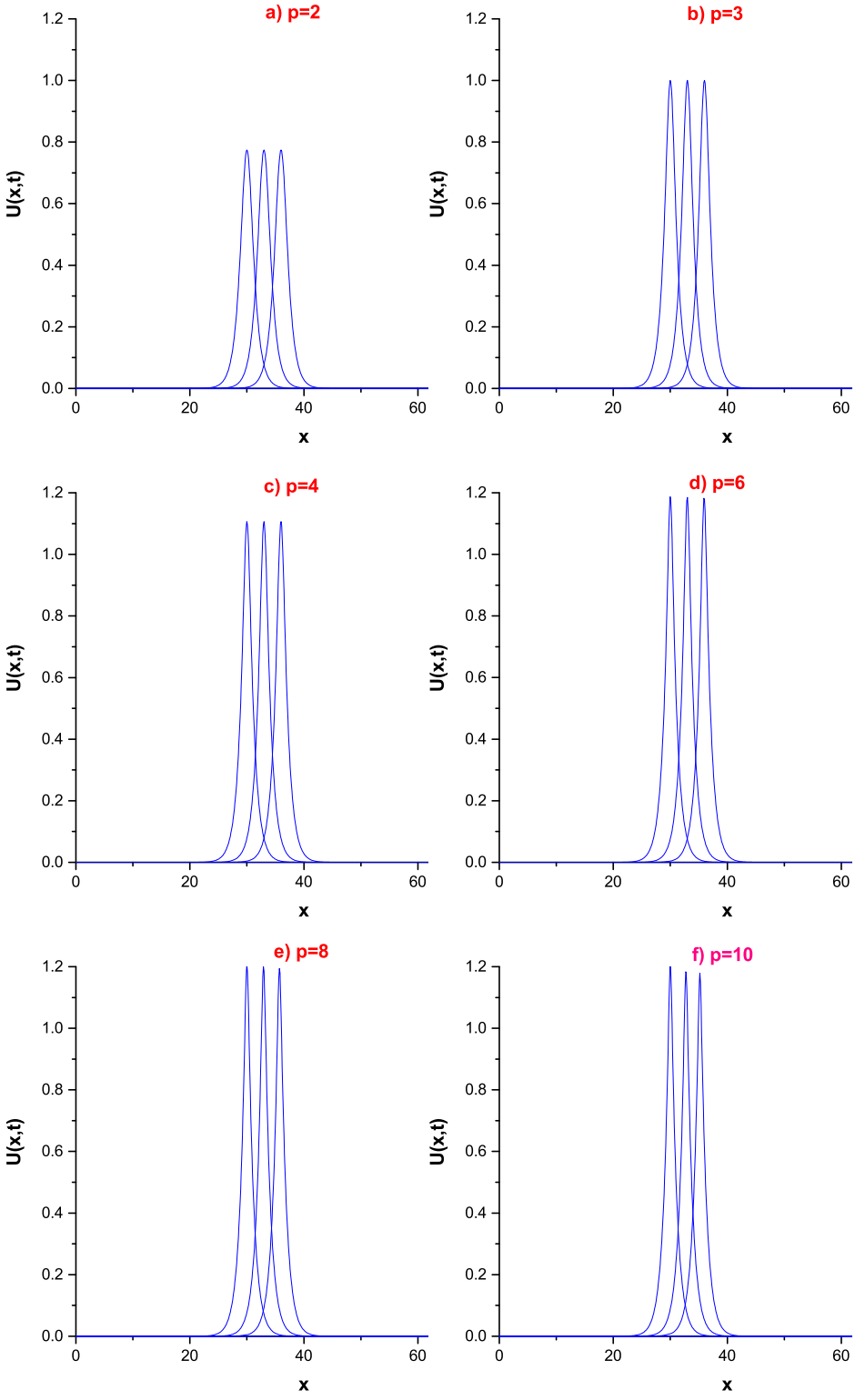

FIG. 4.1. *Single solitary wave with* $c = 0.3, x_0 = 30, x \in [0, 80]$, $t = 0, 10, 20$.

ETNA
Kent State University and
Johann Radon Institute (RICAM)

TABLE 4.7
Errors for single solitary wave with $t = 20, x \in [0, 80]$.

			p=6		p=8		p=10	
		c	0.03	0.1	0.03	0.1	0.03	0.1
		amp	0.80	0.98	0.90	1.05	0.95	1.08
	h	Δt						
	0.1	0.01	0.015	0.036	0.042	0.095	0.102	0.261
	0.2	0.01	0.438	1.192	2.657	9.556	16.085	59.734
$L_2 \times 10^3$	0.1	0.05	0.016	0.071	0.042	0.158	0.103	0.384
	0.2	0.05	0.438	1.224	2.658	9.626	16.088	59.918
	0.1	0.2	0.023	0.813	0.054	2.066	0.125	5.460
	0.1	0.01	0.024	0.031	0.062	0.091	0.143	0.252
	0.2	0.01	0.678	1.142	3.062	8.212	14.057	47.756
$L_\infty \times 10^3$	0.1	0.05	0.024	0.058	0.063	0.141	0.144	0.350
	0.2	0.05	0.678	1.169	3.063	8.262	14.059	47.886
	0.1	0.2	0.030	0.643	0.073	1.731	0.160	4.742

TABLE 4.8
Comparison of results for the single solitary wave with $h = 0.1, \Delta t = 0.2, t = 20, x \in [0, 80]$.

	Methods	$L_2 \times 10^3$	$L_\infty \times 10^3$	I_1	I_2	I_3
$p = 2$	CubBSC[21]	0.19588	0.17443	0.78466	0.16643	0.00519
$c = 1/32$	QuadBSC[4]	0.15695	0.20214	0.78528	0.16658	0.00520
	QuadBSLG[3]	0.08100	0.04596			
	CubBSLG[12]	0.07833	0.04448			
	QuadBSPG[24]	0.00250	0.00275	0.78539	0.16666	0.00520
	QuarBSC[10]	0.00157	0.00104	0.78539	0.16666	0.00520
	Ours-QuinBSC	0.00135	0.00091	0.78539	0.16666	0.00520
$p = 3$	CubBSC[21]	0.514967	0.320605	0.65908	0.05938	0.000068
$c = 0.001$	QuadBSPG[24]	0.000064	0.000082	0.41891	0.05497	0.000073
	Ours-QuinBSC	0.000019	0.000023	0.41891	0.05498	0.000073
$p = 4$	QuadBSPG[24]	2.30499	1.88285	2.62206	2.35615	0.78534
$c = 0.2$	Ours-QuinBSC	3.39086	2.47031	2.62192	2.35593	0.78513

and 0.002%. Moreover, the obtained results are in good agreement with the ones computed by the Petrov-Galerkin scheme [24].

In the second case, we choose the parameters $p = 3$, $c_1 = 0.3$, and $c_2 = 0.0375$. The computer program is run until time $t = 100$. The obtained results are given in Table 4.10. It is observed from Table 4.10 that the variations of the invariants from their initial state are less than 0.0002%, 0.0005%, and 0.0006%, respectively. The numerical values of the invariants are also found to be very close to those of Roshan [24]. The motion of two solitary waves is plotted at different times in Figure 4.2. In this figure, initially, the wave with larger amplitude is located to the left of the second wave with smaller amplitude. As time increases, the interaction starts and the overlapping process occurs. After time $t = 50$, the waves start to resume their original forms.

ETNA
Kent State University and
Johann Radon Institute (RICAM)

TABLE 4.9
Invariants for interaction of two solitary waves with $p = 2, c_1 = 0.5, c_2 = 0.125, x_1 = 15, x_2 = 30, h = 0.1, \Delta t = 0.025$.

	t	0	10	20	30	40	50	60
I_1	Ours-First	4.71237	4.71237	4.71237	4.71237	4.71237	4.71237	4.71237
	Ours-Second	4.71237	4.71237	4.71237	4.71236	4.71237	4.71237	4.71237
	PG[24]	4.71239	4.71239	4.71239	4.71239	4.71239	4.71239	4.71239
I_2	Ours-First	3.33332	3.33332	3.33332	3.33332	3.33332	3.33332	3.33332
	Ours-Second	3.33332	3.33332	3.33332	3.33331	3.33332	3.33332	3.33332
	PG[24]	3.33324	3.33324	3.33324	3.33324	3.33333	3.33338	3.33333
I_3	Ours-First	1.41666	1.41666	1.41666	1.41665	1.41666	1.41666	1.41666
	Ours-Second	1.41666	1.41666	1.41666	1.41664	1.41665	1.41666	1.41666
	PG[24]	1.14166	1.14166	1.14166	1.14166	1.14166	1.14166	1.14166

TABLE 4.10
Invariants for interaction of two solitary waves with $p = 3, c_1 = 0.3, c_2 = 0.0375, x_1 = 15, x_2 = 30, h = 0.1, \Delta t = 0.025$.

	t	0	10	20	40	60	80	90	100
I_1	Ours-First	4.20653	4.20653	4.20653	4.20653	4.20653	4.20653	4.20653	4.20653
	Ours-Sec.	4.20653	4.20653	4.20653	4.20653	4.20653	4.20653	4.20653	4.20653
	PG[24]	4.20655	4.20655	4.20655	4.20655	4.20655	4.20655	4.20655	4.20655
I_2	Ours-First	3.07988	3.07988	3.07988	3.07988	3.07988	3.07988	3.07988	3.07988
	Ours-Sec.	3.07988	3.07988	3.07988	3.07988	3.07988	3.07988	3.07988	3.07988
	PG[24]	3.97977	2.07986	3.07982	3.07986	3.07987	3.07991	3.07974	3.07972
I_3	Ours-First	1.01636	1.01636	1.01636	1.01636	1.01636	1.01636	1.01636	1.01636
	Ours-Sec.	1.01636	1.01636	1.01636	1.01635	1.01635	1.01636	1.01636	1.01636
	PG[24]	1.01634	1.01634	1.01634	1.01634	1.01633	1.01633	1.01633	1.01634

Finally, we consider the parameters $p = 4$, $c_1 = 0.2$, and $c_2 = 1/80$. The experiments are run from time $t = 0$ to time $t = 120$. The calculated quantities of the invariants are presented in Table 4.11. As can be seen in Table 4.11, the deviations of the invariants from their initial values are less than 0.0003%, 0.0007%, and 0.0007%, respectively. The invariant values are compatible with those of Roshan [24]. The interaction of two solitary waves is simulated at different time levels in Figure 4.3, which shows that the initial position of the wave with larger amplitude is on the left of the second wave with smaller amplitude. The interaction starts at time $t = 50$. In progress of time, the overlapping process occurs. After time $t = 70$, the waves start to resume their original shapes.

4.3. A Maxwellian initial condition. In the last test problem, equation (1.1) is supplemented by the following Maxwellian initial condition

$$U(x, 0) = \exp(-x^2), \qquad -20 \le x \le 20.$$

When examining the numerical results with the Maxwellian initial condition given in [4, 10, 20, 24], it can be observed that the choice of μ affects the behaviour of the solution. Hence, we choose different values of $\mu = 0.01$, $\mu = 0.025$, $\mu = 0.05$, $\mu = 0.1$, for $p = 2, 3, 4$. The

ETNA
Kent State University and
Johann Radon Institute (RICAM)

TABLE 4.11
Invariants for interaction of two solitary waves with $p = 4, c_1 = 0.2, c_2 = 1/80, x_1 = 15, x_2 = 30, h = 0.1, \Delta t = 0.025$.

	t	0	10	20	40	60	80	100	120
I_1	Ours-First	3.93307	3.93307	3.93307	3.93307	3.93307	3.93307	3.93307	3.93307
	Ours-Sec.	3.93307	3.93307	3.93307	3.93307	3.93307	3.93307	3.93307	3.93307
	PG[24]	3.93309	3.93309	3.93309	3.93309	3.93309	3.93309	3.93309	3.93309
I_2	Ours-First	2.94524	2.94524	2.94524	2.94524	2.94524	2.94524	2.94523	2.94523
	Ours-Sec.	2.94524	2.94524	2.94523	2.94523	2.94523	2.94523	2.94523	2.94523
	PG[24]	2.94512	2.94518	2.94517	2.94515	2.94505	2.94506	2.94508	2.94511
I_3	Ours-First	0.79766	0.79766	0.79766	0.79766	0.79766	0.79766	0.79766	0.79766
	Ours-Sec.	0.79766	0.79766	0.79766	0.79766	0.79766	0.79766	0.79766	0.79766
	PG[24]	0.79761	0.79761	0.79761	0.79761	0.79762	0.79761	0.79761	0.79761

TABLE 4.12
Invariants for Maxwellian initial condition.

μ	t	$p=2$			$p=3$			$p=4$		
		I_1	I_2	I_3	I_1	I_2	I_3	I_1	I_2	I_3
0.01	0	1.7724	1.2658	0.8862	1.7724	1.2658	0.7926	1.7724	1.2658	0.7236
	4	1.7732	1.2678	0.9061	1.7786	1.2847	0.8782	1.7855	1.2931	0.7715
	8	1.7742	1.2736	0.9234	1.7868	1.3131	0.9691	1.8014	1.3622	1.2362
	12	1.7739	1.2711	0.9123	1.7813	1.2901	0.8664	1.8156	1.3901	1.2707
PG[24]	12	1.7724	1.2658	0.8862	1.7724	1.2665	0.7947	1.7725	1.2669	0.7253
0.025	0	1.7724	1.2846	0.8862	1.7724	1.2846	0.7926	1.7724	1.2846	0.7236
	4	1.7725	1.2846	0.8880	1.7731	1.2863	0.8056	1.7763	1.2967	0.7891
	8	1.7725	1.2846	0.8881	1.7733	1.2859	0.7996	1.7711	1.2762	0.7129
	12	1.7725	1.2846	0.8881	1.7730	1.2837	0.7946	1.7791	1.3056	0.8198
PG[24]	12	1.7724	1.2835	0.8856	1.7723	1.2834	0.7910	1.7724	1.2849	0.7243
0.05	0	1.7724	1.3159	0.8862	1.7724	1.3159	0.7926	1.7724	1.3159	0.7236
	4	1.7724	1.3159	0.8864	1.7725	1.3159	0.7938	1.7726	1.3155	0.7253
	8	1.7724	1.3159	0.8864	1.7725	1.3159	0.7939	1.7729	1.3168	0.7297
	12	1.7724	1.3159	0.8864	1.7725	1.3160	0.7940	1.7735	1.3188	0.7345
PG[24]	12	1.7724	1.3160	0.8861	1.7724	1.3156	0.7922	1.7724	1.3177	0.7245
0.1	0	1.7724	1.3786	0.8862	1.7724	1.3786	0.7926	1.7724	1.3786	0.7236
	4	1.7724	1.3786	0.8862	1.7724	1.3786	0.7928	1.7725	1.3786	0.7243
	8	1.7724	1.3786	0.8862	1.7724	1.3786	0.7928	1.7725	1.3787	0.7243
	12	1.7724	1.3786	0.8862	1.7724	1.3786	0.7928	1.7725	1.3786	0.7243
PG[24]	12	1.7724	1.3785	0.8861	1.7724	1.3787	0.7926	1.7734	1.3836	0.7224

numerical calculations of the three invariants are done up to time $t = 12$, and the results are recorded in Table 4.12. From this table, we can easily see that as the value of μ increases, the variations of the invariants become smaller and remain less than 0.08%. The evolution of the Maxwellian initial condition at $t = 12$ is depicted for different values of μ in Figure 4.4 and Figure 4.5. It is clearly seen in these figures that when the value of μ decreases, the number of the stable solitary wave increases.

5. Conclusion. In this work, the quintic B-spline collocation method with two different linearization techniques was employed to obtain the numerical solution of the GEW equation. Our numerical scheme has been tested by applying three test problems including a single solitary wave, the interaction of two solitary waves, and a Maxwellian initial condition. The

ETNA
Kent State University and
Johann Radon Institute (RICAM)

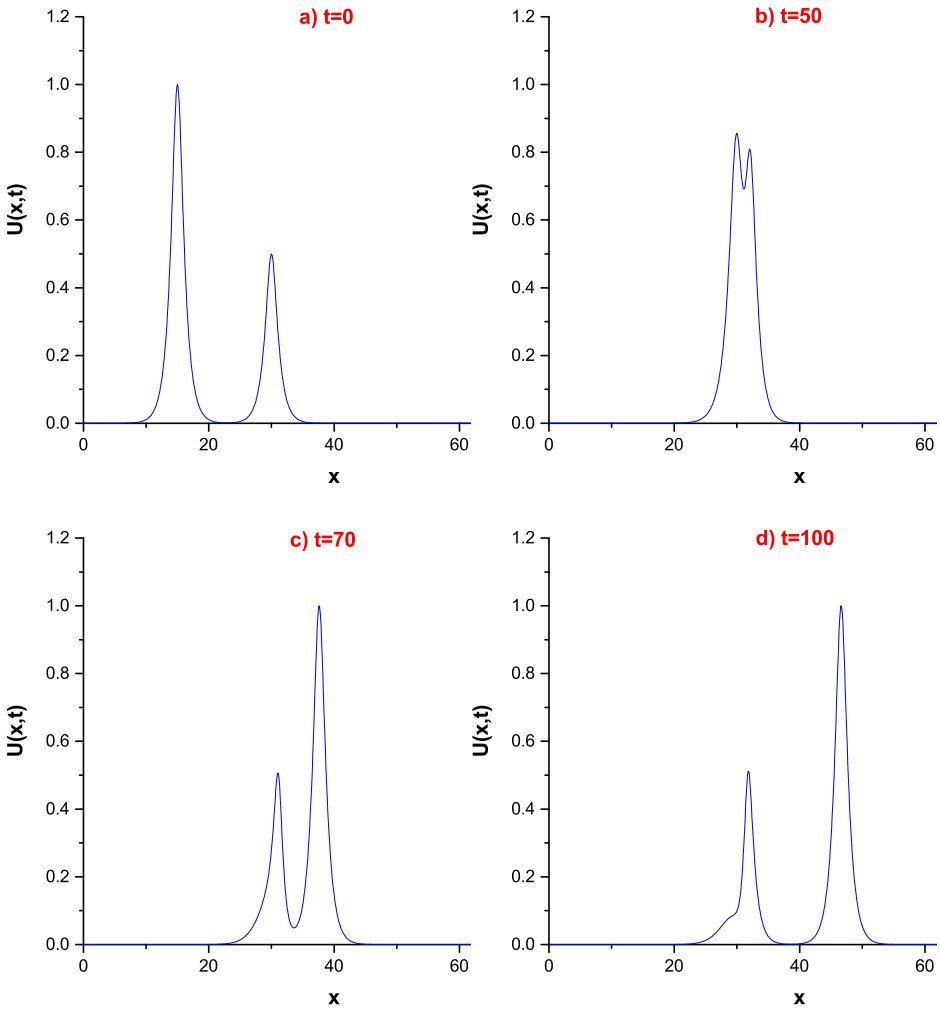

FIG. 4.2. *Interaction of two solitary waves at* $p = 3$.

error in the L_2 and L_∞-norms and three conservative quantities, I_1, I_2, and I_3, have been computed to demonstrate the performance of the algorithm. The calculated data show that the numerical value of the invariants is nearly constant during the iterations and is consistent with earlier results. The magnitude of our error norms is found to be sufficiently small. As listed in Table 4.6 and Table 4.7, if the space and time gridsize are reduced, the presented scheme is capable of producing better results. According to the comparison in Table 4.8, our calculated error norms are smaller than the ones in existing collocation methods [21, 4, 10], Galerkin methods [3, 12], and Petrov-Galerkin method [24] based on B-splines. Also, it can be seen from the figures that the numerical results reproduce the motion of solitary waves and solitons as expected. This means that the proposed algorithm is a successful and efficient numerical technique for solving the GEW equation.

6. Acknowledgements. The authors would like to express their sincere thanks to the reviewers for their careful reading, valuable comments, and suggestions.

ETNA
Kent State University and
Johann Radon Institute (RICAM)

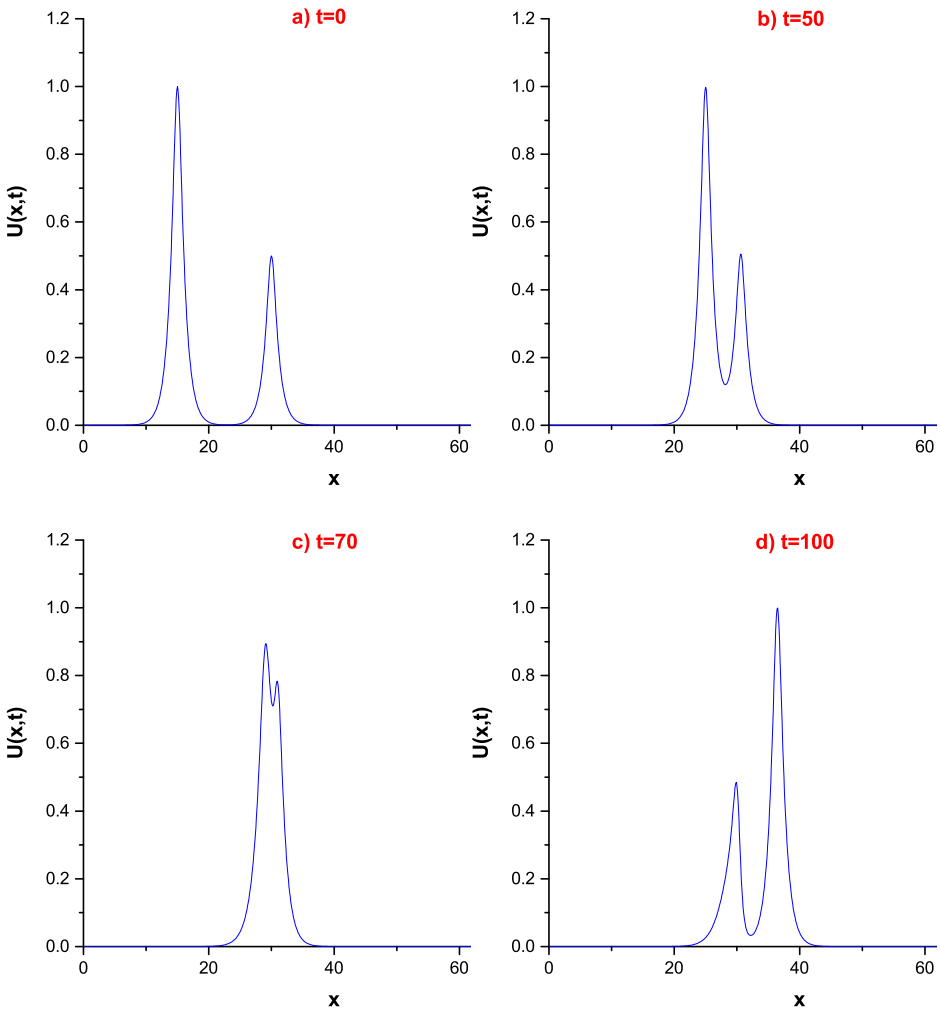

FIG. 4.3. *Interaction of two solitary waves at* $p = 4$.

REFERENCES

[1] T. B. BENJAMIN, J. L. BONA, AND J. J. MAHONY, *Model equations for long waves in non-linear dispersive systems*, Philos. Trans. Roy. Soc. London Ser. A, 272 (1972), pp. 47–78.
[2] İ. DAĞ AND B. SAKA, *A cubic B-spline collocation method for the EW equation*, Math. Comput. Appl., 9 (2004), pp. 381–392.
[3] A. ESEN, *A lumped Galerkin method for the numerical solution of the modified equal-width wave equation using quadratic B-splines*, Int. J. Comput. Math., 83 (2006), pp. 449–459.
[4] D. J. EVANS AND K. R. RASLAN, *Solitary waves for the generalized equal width (GEW) equation*, Int. J. Comput. Math., 82 (2005), pp. 445–455.
[5] F. FAZAL-I HAQ, I. A. SHAH, AND S. AHMAD, *Septic B-spline collocation method for numerical solution of the equal width wave (EW) equation*, Life Sci. J., 10 (1s) (2013), pp. 253–260.
[6] L. R. T. GARDNER AND G. A. GARDNER, *Solitary waves of the equal width wave equation*, J. Comput. Phys., 101 (1992), pp. 218–223.
[7] L. R. T. GARDNER, G. A. GARDNER, F. A. AYOUP, AND N. K. AMEIN, *Simulations of the EW undular bore*, Commun. Numer. Meth. Engng., 13 (1997), pp. 583–592.
[8] T. GEYIKLI AND S. B. G. KARAKOC, *Septic B-spline collocation method for the numerical solution of the*

ETNA
Kent State University and
Johann Radon Institute (RICAM)

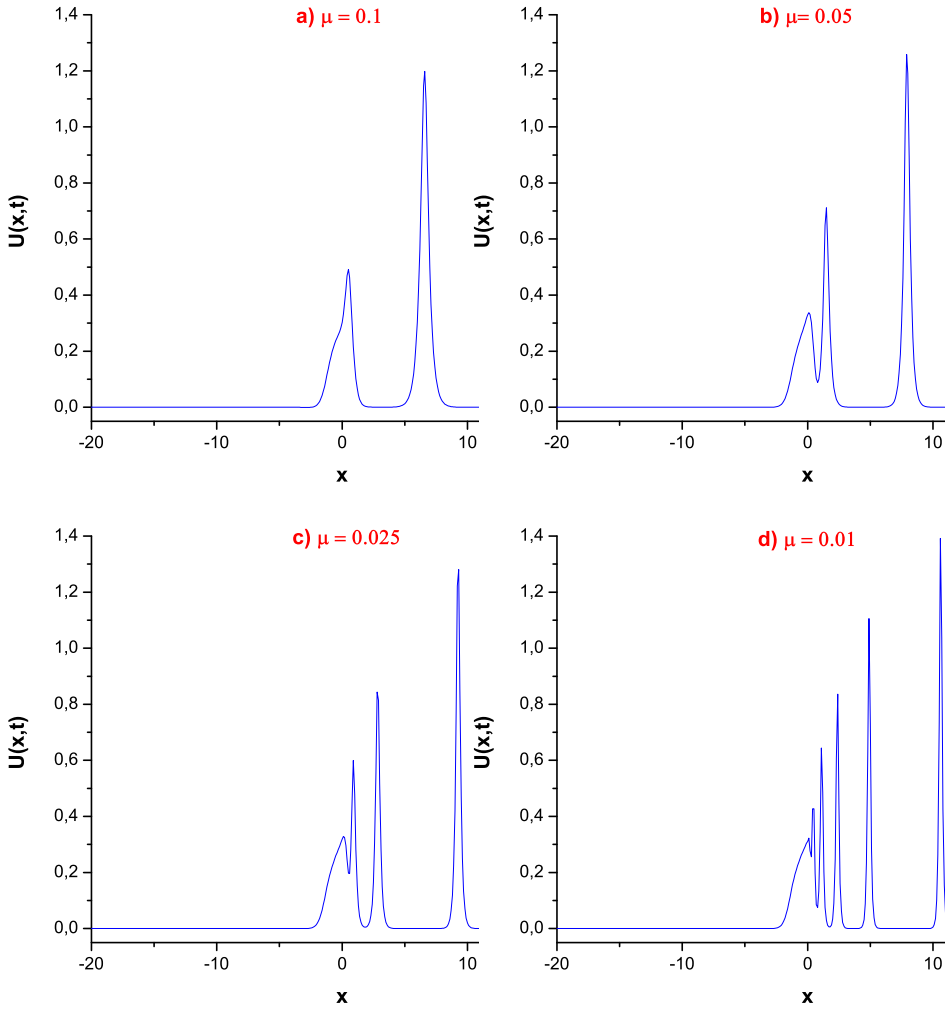

FIG. 4.4. *Maxwellian initial condition* $p = 3$ *at* $t = 12$.

modified equal width wave equation, Appl. Math. (Irvine), 2 (2011), pp. 739–749.

[9] S. HAMDI, W. H. ENRIGHT, W. E. SCHIESSER, AND J. J. GOTTLIEB, *Exact solutions of the generalized equal width wave equation*, in Computational Science and its Applications—ICCSA 2003. Part II, V. Kumar, M. L. Gavrilova, C. J. K. Tan, and P. L' Ecuyer, eds. Lecture Notes in Comput. Sci. 2668, Springer, Berlin, 2003, pp. 725–734.

[10] S. İSLAM, F. HAQ, AND I. A. TIRMIZI, *Collocation method using quartic B-spline for numerical solution of the modified equal width wave equation*, J. Appl. Math. Inform., 28 (2010), pp. 611–624.

[11] S. B. G. KARAKOÇ, T. AK, AND H. ZEYBEK, *An efficient approach to numerical study of the MRLW equation with B-spline collocation method*, Abstr. Appl. Anal., (2014), Art. ID 596406 (15 pages).

[12] S. B. G. KARAKOÇ AND T. GEYIKLI, *Numerical solution of the modified equal width wave equation*, Int. J. Differ. Equ., (2012), Art. ID 587208 (15 pages).

[13] S. B. G. KARAKOC, N. M. YAGMURLU, AND Y. UCAR, *Numerical approximation to a solution of the modified regularized long wave equation using quintic B-splines*, Bound. Value Probl., 2013, Art. ID 2013:27 (17 pages).

[14] S. B. G. KARAKOÇ, H. ZEYBEK, AND T. AK, *Numerical solutions of the Kawahara equation by the septic B-spline collocation method*, Stat. Optim. Inf. Comput., 2 (2014), pp. 211–221.

[15] A. K. KHALIFA, K. R. RASLAN, AND H. M. ALZUBAIDI, *A collocation method with cubic B-splines for*

ETNA
Kent State University and
Johann Radon Institute (RICAM)

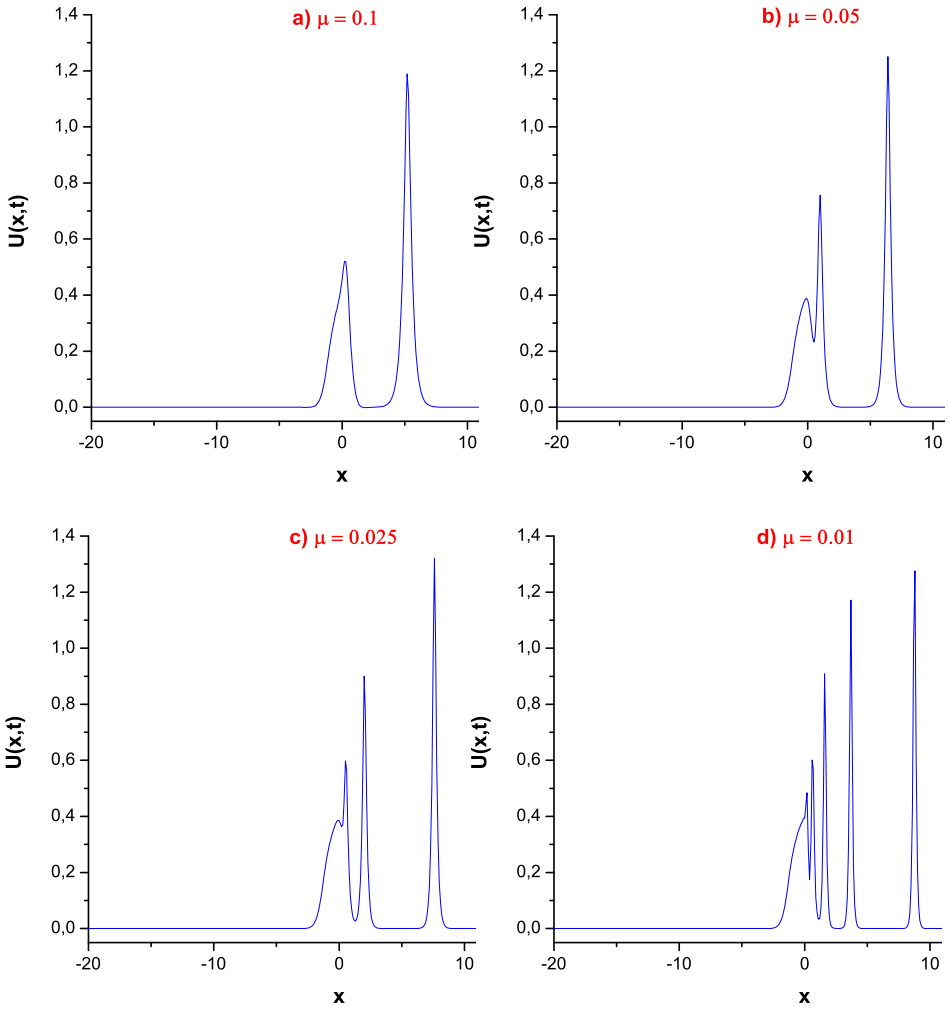

FIG. 4.5. *Maxwellian initial condition* $p = 4$ *at* $t = 12$.

solving the MRLW equation, J. Comput. Appl. Math., 212 (2008), pp. 406–418.

[16] R. C. MITTAL AND R. K. JAIN, *Numerical solution of general Rosenau-RLW equation using quintic B-splines collocation method*, Commun. Numer. Anal., 2012, Art. ID 00129 (16 pages).

[17] H. PANAHIPOUR, *Numerical simulation of GEW equation using RBF collocation method*, Commun. Numer. Anal., 2012, Art. ID 00059 (28 pages).

[18] D. H. PEREGRINE, *Long waves on a beach*, J. Fluid Mech., 27 (1967), pp. 815–827.

[19] P. M. PRENTER, *Splines and Variational Methods*, Wiley, New York, 1975.

[20] K. R. RASLAN, *Collocation method using quartic B-spline for the equal width (EW) equation*, Appl. Math. Comput., 168 (2005), pp. 795–805.

[21] ———, *Collocation method using cubic B-spline for the generalised equal width equation*, Int. J. Simul. Proc. Modelling, 2 (2006), pp. 37–44.

[22] K. R. RASLAN AND T. S. EL-DANAF, *Solitary waves solutions of the mrlw equation using quintic B-splines*, J. King Saud Univ. Sci., 22 (2010), pp. 161–166.

[23] K. R. RASLAN, T. S. EL-DANAF, AND K. K. ALI, *Collocation method with quintic B-spline method for solving Hirota-Satsuma coupled KdV equation*, Int. J. Appl. Math. Res., 5, (2016), pp. 123–131.

[24] T. ROSHAN, *A Petrov-Galerkin method for solving the generalized equal width (GEW) equation*, J. Comput. Appl. Math., 235 (2011), pp. 1641–1652.

ETNA
Kent State University and
Johann Radon Institute (RICAM)

[25] S. G. RUBIN AND R. A. GRAVES, *A cubic spline approximation for problems in fluid mechanics*, Tech. Report, NASA TR R–436, NASA Research Center, Hampton, 1975.
[26] B. SAKA, *Algorithms for numerical solution of the modified equal width wave equation using collocation method*, Math. Comput. Modelling, 45 (2007), pp. 1096–1117.
[27] B. SAKA, İ. DAĞ, AND D. IRK, *Quintic B-spline collocation method for numerical solution of the RLW equation*, ANZIAM J., 49 (2008), pp. 389–410.
[28] A. A. SOLIMAN AND M. H. HUSSIEN, *Collocation solution for RLW equation with septic spline*, Appl. Math. Comput., 161 (2005), pp. 623–636.
[29] N. TAGHIZADEH, M. MIRZAZADEH, M. AKBARI, AND M. RAHIMIAN, *Exact solutions for generalized equal width equation*, Math. Sci. Lett., 2 (2013), pp. 99–106.
[30] S. I. ZAKI, *A least-squares finite element scheme for the EW equation*, Comp. Methods Appl. Mech. Engrg., 189 (2000), pp. 587–594.
[31] ———, *A quintic B-spline finite elements scheme for the KdVB equation*, Comp. Methods Appl. Mech. Engrg., 188 (2000), pp. 121–134.